



**HAL**  
open science

# Acetyl Methyl Torsion in Pentan-2-one As Observed by Microwave Spectroscopy

Maike Andresen, Isabelle Kleiner, Martin Schwell, Wolfgang Stahl, Ha Vinh  
Lam Nguyen

► **To cite this version:**

Maike Andresen, Isabelle Kleiner, Martin Schwell, Wolfgang Stahl, Ha Vinh Lam Nguyen. Acetyl Methyl Torsion in Pentan-2-one As Observed by Microwave Spectroscopy. *Journal of Physical Chemistry A*, 2018, 122 (35), pp.7071-7078. 10.1021/acs.jpca.8b06183 . hal-03183068

**HAL Id: hal-03183068**

**<https://hal.science/hal-03183068>**

Submitted on 26 Mar 2021

**HAL** is a multi-disciplinary open access archive for the deposit and dissemination of scientific research documents, whether they are published or not. The documents may come from teaching and research institutions in France or abroad, or from public or private research centers.

L'archive ouverte pluridisciplinaire **HAL**, est destinée au dépôt et à la diffusion de documents scientifiques de niveau recherche, publiés ou non, émanant des établissements d'enseignement et de recherche français ou étrangers, des laboratoires publics ou privés.

# Acetyl Methyl Torsion in Pentan-2-one as Observed by Microwave Spectroscopy

*Maike Andresen,<sup>a,b</sup> Isabelle Kleiner,<sup>b</sup> Martin Schwell,<sup>b</sup> Wolfgang Stahl,<sup>a</sup> and Ha Vinh Lam  
Nguyen<sup>b\*</sup>*

<sup>a</sup> Institute of Physical Chemistry, RWTH Aachen University, Landoltweg 2, D-52074 Aachen,  
Germany

<sup>b</sup> Laboratoire Interuniversitaire des Systèmes Atmosphériques (LISA), CNRS UMR 7583,  
Université Paris-Est Créteil, Université Paris Diderot, Institut Pierre Simon Laplace, 61  
avenue du Général de Gaulle, F-94010 Créteil, France

## ABSTRACT

The rotational spectra of two conformers of pentan-2-one (also known as methyl propyl ketone) were recorded in the frequency range from 2 to 40 GHz using two molecular jet Fourier transform microwave spectrometers. Fine splittings due to the internal rotations of the acetyl methyl group  $\text{CH}_3\text{CO}-$  and the butyryl methyl group  $-\text{COCH}_2\text{CH}_2\text{CH}_3$  were resolved and analyzed with high accuracy. The torsional barriers of the acetyl and the butyryl methyl groups are  $238.14\text{ cm}^{-1}$  and  $979\text{ cm}^{-1}$ , respectively, for the lowest energy conformer, as well as  $188.384\text{ cm}^{-1}$  and  $1032\text{ cm}^{-1}$ , respectively, for the other one. From the results obtained for the acetyl methyl group, a general rule to predict its torsional barrier in ketones based on the molecular symmetry is proposed.

## INTRODUCTION

Fourier transform microwave spectroscopy has become the most important method to investigate the large amplitude motions (LAMs) of a molecule, where internal rotation is one of the main fields of interest. Due to higher resolution and more accurately determined molecular parameters in comparison to for example fluorescence or electronic spectroscopy, many barriers to internal rotations have been investigated by this method. The effect of internal rotation, in the most frequent cases of methyl groups, causes all rotational transitions in the spectrum to split into multiplets. The width of these splittings depends on the respective rotational state, the orientations of the methyl groups in the molecule, and the barriers to internal rotation. In many cases, the barrier heights of internal rotors can be linked to functional groups and other structural characteristics of the molecule, making the internal rotation top a spectroscopic “detector” of structure. For example, systematic microwave spectroscopic studies on a series of *n*-alkyl acetates, starting with methyl acetate up to *n*-hexyl acetate, have proven that the barrier to internal rotation of the acetyl methyl group is always around  $100\text{ cm}^{-1}$ .<sup>1-6</sup> In contrast, a number of ketones containing an acetyl methyl group have been investigated in the literature, but no conclusive trends could be determined concerning the barrier to internal rotation.<sup>7</sup> The barrier heights vary in a wide range from about  $170\text{ cm}^{-1}$  to  $440\text{ cm}^{-1}$ . One of the lowest barrier heights has been found in methyl neopentyl ketone with a value of  $174.1\text{ cm}^{-1}$ ,<sup>8</sup> while the value of  $433.8\text{ cm}^{-1}$  detected in anti-periplanar methyl vinyl ketone belongs to the highest values in this range.<sup>9</sup> Currently, no systematic microwave spectroscopic studies on ketones exist to state a general rule to explain the difference of the barriers.

Predicting the barriers to internal rotation is a difficult task, since chemical intuition often fails and quantum chemistry is not yet sufficiently accurate at experimental level. While a deviation of  $1\text{ kJ}\cdot\text{mol}^{-1}$  (about  $84\text{ cm}^{-1}$ ) already indicates a very high quality of the calculations, the difference is tremendous in the microwave spectra. If the barrier height is

low, a deviation of  $1\text{ cm}^{-1}$  of its value might lead to a shift of the experimental transitions by hundreds of MHz.

Methyl propyl ketone (MPK), also known as pentan-2-one, is a volatile, colorless liquid. Regarding its LAMs, it features an acetyl methyl group and a butyryl methyl group which undergo internal rotation. For a systematic investigation on the LAMs in ketone physics, MPK is a key molecule to study, because it belongs to the series of saturated methyl alkyl ketones, where the two first members acetone<sup>10</sup> and methyl ethyl ketone<sup>11</sup> have already been thoroughly investigated. MPK is the next member in line. The results obtained from the LAMs of MPK would provide new insights and could reveal at least a part of the almost unknown behavior of barrier heights in ketones.

MPK combines an acetyl methyl group with an alkyl chain sufficiently long to support conformational isomers. The goal is to determine the preferred conformations of this substance as a necessary first step in subsequent studies on determining the barrier height in each conformer. Regarding the internal dynamics of MPK, it was expected that torsional splittings arising from the internal rotation of the acetyl methyl group,  $\text{CH}_3\text{CO}-$ , could be resolved in the experimental spectrum, as has been observed in other linear aliphatic ketones previously studied.<sup>10,11</sup>

The same kind of LAM as for the acetyl methyl group is found for the butyryl methyl group  $-\text{COCH}_2\text{CH}_2\text{CH}_3$  at the end of the alkyl chain. Its barrier height is estimated to be about  $1000\text{ cm}^{-1}$ , similar to that of the ethyl methyl group in diethyl amine.<sup>12</sup> As described in the section on the *Microwave Spectrum*, the splittings arising from this LAM are also resolvable with our experimental setup.

In nature, MPK is found as a pheromone compound of honey bees.<sup>13</sup> Pheromones are signals of chemical information systems, which trigger behavioral changes, especially in insects, for example to mark territory or aliment, and to regulate the social system.<sup>14</sup> Some

insect species release alarm pheromones during an attack to trigger either escape or increased aggression. In honey bees, this kind of pheromone is a complex mixture containing several tens of different compounds with a vast amount of acetates and methyl alkyl ketones, such as isoamyl acetate, hexyl acetate, octyl acetate, heptanone, and pentanone (the molecule investigated in this work).<sup>13,15,16</sup> Pheromones are often detected in olfactory receptors. The study of olfactory is complex and requires the interplay between chemistry, biology, and theoretical calculations to approach the problems. From the chemical side, the geometries of pheromones provide interesting questions concerning their conformational orientation: How does molecular shape fit together in the insect receptors? Can information on the olfaction membrane binding site be extracted from the structures of the pheromones? To thoroughly investigate the structure and dynamic of pheromone compounds at a molecular level might be helpful to answer these questions in the future. The interplay between microwave spectroscopy and quantum chemistry currently presents an optimal combination to determine the gas phase structure and the internal dynamic of a pheromone substance.

## THEORETICAL METHODS

**Internal Rotations.** MPK has two inequivalent methyl rotors, the acetyl and butyryl methyl groups. Each rotational transition of such a molecule splits into five torsional species labelled as  $(\sigma_1\sigma_2) = (00), (01), (10), (11)$  and  $(12)$ .<sup>17</sup> The numbers  $\sigma = 0, 1, 2$  represent the three symmetry species A, E<sub>a</sub>, E<sub>b</sub> of the C<sub>3</sub> groups of the internal rotors, respectively. They correspond to the transformation properties of the C<sub>3</sub>-adapted planar rotor wave functions  $e^{i(3k+\sigma)\varphi}$  with  $k \in \mathbb{Z}$  and the torsional angle  $\varphi$ . In this notation,  $\sigma_1$  refers to the acetyl methyl group and  $\sigma_2$  to the butyryl methyl group.

## Quantum Chemical Calculations.

**Conformational Analysis.** With continuously increasing computer capability, quantum chemistry has become a powerful tool to predict stable conformers and barrier heights of large molecules, and thus offers an excellent interplay with microwave spectroscopy, which yields accurate experimental parameters serving as benchmark tests for the calculated values.

To obtain possible conformers of MPK, we created various starting geometries by setting the dihedral angles  $\alpha_1 = \angle(\text{C}_1, \text{C}_5, \text{C}_7, \text{C}_{10})$  and  $\alpha_2 = \angle(\text{C}_5, \text{C}_7, \text{C}_{10}, \text{C}_{13})$  (for atom numbering see Figure 1) to  $180^\circ$ ,  $60^\circ$  and  $-60^\circ$ , and optimized all geometry parameters including  $\alpha_1$  and  $\alpha_2$ . The dihedral angle  $\varphi(\text{A}, \text{B}, \text{C}, \text{D})$  is defined as the angle between the ABC plane and the BCD plane. When looking from B to C, a clockwise rotation refers to a positive angle, while the value is negative for the counter clockwise direction. The rotations about the  $\text{C}_1\text{--}\text{C}_5$  and  $\text{C}_{10}\text{--}\text{C}_{13}$  axes are equivalent to the internal rotations of the acetyl and butyryl methyl groups, respectively, and do not create new conformations. The nine starting geometries were optimized to a local energy minimum at the MP2/6-311++G(d,p) level of theory using the *Gaussian09* package,<sup>18</sup> yielding four conformers, which are illustrated in Figure 2. This level of theory was chosen, since it calculated rotational constants close to the experimental ones in many of our previous works.<sup>19-21</sup> Additional harmonic frequency calculations proved that all of the conformers are stable ones and not saddle points. The calculated energies, rotational constants, dipole moment components and optimized dihedral angles  $\alpha_1$  and  $\alpha_2$  are listed in Table 1. The nuclear coordinates in the principal axis system of all conformers are available in Table S1 in the Electronic Supporting Information (ESI).

The global minimum conformer, conformer I, occurs at  $(\alpha_1, \alpha_2) = (161.4, -69.5^\circ)$ , see Table 1) and has the butyryl methyl group tilted out of the plane spanned by the  $\text{C}_1$ ,  $\text{C}_5$ ,  $\text{O}_6$ ,  $\text{C}_7$  atoms (which make up the acetyl group). Similar structures where the  $\gamma$ -carbon is in a nearly synclinal position have been observed for molecules containing a propyl group, such as *n*-

propyl acetate<sup>3</sup> and methyl butyrate.<sup>22</sup> For the former molecule, the tilt angle is 63.0° and for the latter 68.5°.

The conformer with the second lowest energy (called conformer II) seems to possess C<sub>s</sub> symmetry, but a closer look at the structure reveals that the real symmetry is not C<sub>s</sub>. The propyl chain is tilted out of the C<sub>s</sub> plane at the  $\alpha$ -carbon position by an angle of about 10° ( $\alpha_1 = 170.1^\circ$ , see Table 1). This “pseudo-C<sub>s</sub>” structure has been frequently observed in previous investigations on aliphatic ketones. For example, a tilt angle out of the C–(C=O)–C plane of about 10° was calculated for each ethyl group in diethyl ketone.<sup>23</sup> A similar tilt angle was found for the *tert*-butyl group in methyl neopentyl ketone<sup>8</sup> and the ethyl group in methyl ethyl ketone,<sup>11</sup> while pinacolone features a larger tilt angle of 16°.<sup>24</sup>

The two other conformers, conformer III and IV, both show a value of  $\alpha_1 \approx \pm 60^\circ$  and are about 2 and 4 kJ mol<sup>-1</sup>, respectively, higher in energy than conformer I. We expected that they cannot be observed in the microwave spectrum under the molecular jet conditions described in the section on the *Experimental Setup* and therefore, we did not consider them for the spectral analysis.

**Basis Set Variation.** Full geometry optimizations were first carried out at the MP2/6-311++G(d,p) level. However, since the calculated structures and consequently the rotational constants of the conformers depend strongly on the level of theory in use,<sup>25,26</sup> the optimizations were redone for the two assigned conformers (see the section on the *Spectral Assignments and Fits*) using a series of MP2 and DFT calculations with different basis sets. A comparison of the calculated and the experimental values explores the level of theory that best matches the experimental rotational constants. The results are summarized in Table S2 for conformer I and in Table S3 for conformer II (see ESI) and will be discussed in the section on the *Results and Discussion*.

**Barriers to Internal Rotation.** The barriers to internal rotation of the acetyl and butyryl methyl groups were calculated for the lowest energy conformers, conformer I and II, by varying the dihedral angle  $\varphi_1 = \angle(\text{C}_1, \text{H}_2, \text{C}_5, \text{C}_7)$  and  $\varphi_2 = \angle(\text{C}_7, \text{C}_{10}, \text{C}_{13}, \text{H}_{15})$ , respectively, in  $10^\circ$  increments, while all other parameters were optimized at the MP2/6-311++G(d,p) and B3LYP/6-311++G(d,p) levels of theory. Due to the symmetry of the methyl group a range of only  $120^\circ$  was sufficient. The corresponding energies were parameterized with a one-dimensional Fourier expansion and the resulting coefficients are given in Table S4 and S5 in the ESI.

Figure 3 depicts the potential energy curve of the rotation of the acetyl methyl group of conformer I with a three-fold potential as expected. However, the shape of the curve is not entirely symmetric, and significant contributions of higher order potential terms are necessary. This is due to the fact that any change in the position of the acetyl methyl group significantly influences the position of the  $\beta$ -carbon of the propyl chain and the dihedral angle  $\alpha_1$  changes by up to  $16.1^\circ$  during this methyl rotation. Obviously, the one-dimensional curve is not suitable to fully describe this two-dimensional problem. Nevertheless, it is an easy method to obtain an estimate of the corresponding barrier heights, which are  $229.8 \text{ cm}^{-1}$  and  $168.3 \text{ cm}^{-1}$  calculated with the MP2 and the B3LYP method, respectively.

Figure 4 shows the potential energy curve of the acetyl methyl group of conformer II of MPK, where double minima with small local maxima in between them exist. For a closer investigation of these minima, we reduced the step width of the dihedral angle  $\varphi_1$  to a grid of  $1^\circ$  in a range of  $\pm 20^\circ$  around a local maximum and observed a deviation of the position of the minima from the local maximum of up to  $15^\circ$ . The presence of the double minima is also due to the coupling of the acetyl methyl group with the position of the  $\beta$ -carbon of the alkyl chain. Since conformer II features a pseudo- $C_s$  symmetry with the alkyl chain tilted by about  $10^\circ$  (see the section on the *Conformational Analysis*), the double minimum represents the two

enantiomers of the conformer. The barrier heights calculated at the MP2/6-311++G(d,p) and B3LYP/6-311++G(d,p) levels are 147.6 cm<sup>-1</sup> and 115.7 cm<sup>-1</sup>, respectively.

In contrast, the potential energy curves of the rotation of the butyryl methyl group illustrated in Figure S1 in the ESI show an almost pure  $V_3$  potential for both conformers at all method and basis set combinations. The Fourier coefficients are available in Table S5 in the ESI. The barrier heights calculated at the MP2/6-311++G(d,p) and B3LYP/6-311++G(d,p) levels of theory are 990.9 cm<sup>-1</sup> and 978.9 cm<sup>-1</sup>, respectively, for conformer I, as well as 1111.1 cm<sup>-1</sup> and 1038.0 cm<sup>-1</sup> for conformer II.

**Effective Hamiltonian Methods.** For the analysis of the internal rotation of the acetyl methyl group in MPK, two different programs treating internal rotation were used, the *XIAM* code<sup>27</sup> and the *BELGI* code in its C<sub>s</sub><sup>28</sup> or C<sub>1</sub> version.<sup>29</sup>

The *XIAM* code uses a combination of the principal axis method and the rho axis method, where the Hamilton matrix of each internal rotor is set up in its own rho axis system. After diagonalization, the eigenvalues and torsional integrals are used to set up the Hamilton matrix in the principal axis system. Matrix elements of each internal rotor are added to the Hamilton matrix, which contains the matrix elements of the overall rotation as well. Finally, the rotorsional eigenvalues is obtained after diagonalizing the matrix.

The program *BELGI* in both symmetry versions also uses a two-step diagonalization procedure. Here, both steps are performed in the rho axis system. In the first step the torsional Hamiltonian  $H_T = F(\mathbf{p}_\varphi - \rho\mathbf{P}_a)^2 + V(\alpha)$  is diagonalized in the basis set  $\exp(i[3k+\sigma_1]\alpha)|K\rangle$ ,<sup>30</sup> where  $k$  is an integer ranging from -10 to 10,  $|K\rangle$  is the symmetric top eigenfunction, and  $\sigma_1$  is either 0 for the A species or  $\pm 1$  for the E species.  $V(\alpha)$  is the internal rotation potential function,  $F$  is the internal rotation constant,  $\mathbf{p}_\varphi$  is the internal rotation angular momentum conjugated to the torsional angle  $\varphi$ ,  $\rho$  is the coupling constant between the internal rotation

and the global rotation, and  $\mathbf{P}_a$  is the a component of the total rotational angular momentum. A  $(2k + 1) \times (2k + 1) = 21 \times 21$  Hamiltonian matrix is diagonalized for each  $K$  value and the torsional eigenvalues and eigenvectors are obtained. In the second step, we used a basis set consisting of products of the torsional eigenfunctions, obtained from the first step diagonalization and the symmetric top wavefunctions  $|JK\rangle$  to diagonalize the rest of the terms of the Hamiltonian, i.e.  $H_R$ ,  $H_{cd}$ , and  $H_{int}$  allowed for the  $C_s^{21}$  or  $C_1^{22}$  symmetry. The nine lowest torsional states  $v_t$  are taken to create a matrix of the size  $(2J + 1) \cdot 9 \times (2J + 1) \cdot 9$  associated with the second step.

The program *XIAM* uses the same value of  $k = k_{\max} = 10$ , but only one torsional state is taken into consideration in the Hamiltonian matrix, leading to a  $(2J + 1) \times (2J + 1)$  matrix and increasing significantly the speed of the calculation. The program *BELGI* takes into account explicitly the interaction between the nine lowest torsional states, and is referred to as a global approach,<sup>31</sup> while *XIAM* fits each  $v_t$  state separately. Additionally, a number of higher order terms can be fitted in the *BELGI* code. The difference between the  $C_s$  and  $C_1$  version of this program is that complex matrix elements are allowed for  $C_1$  symmetry. Therefore, the fit can include terms containing imaginary elements such as  $D_{aci}$ , multiplying  $\{\mathbf{P}_a, \mathbf{P}_c\}$ .

A number of previous studies has shown that the *XIAM* code and the *BELGI* codes are complementary.<sup>32,33</sup> While *XIAM* benefits the advantages of its ease of use and speed, in cases with rather low barriers, E species transitions are not always satisfactorily predicted, due to the fact that the interactions between torsional states can be large. An example is vinyl acetate ( $V_3 = 151.5 \text{ cm}^{-1}$ ), where a standard deviation of 92.3 kHz was obtained in a global *XIAM* fit, while the A species fit achieves the measurement accuracy with a deviation of 1.2 kHz.<sup>34</sup> Using the *BELGI-C<sub>s</sub>* code, both A and E species were fitted to a rms deviation of 2.9 kHz. The same observation is found for conformer I and in some extend for conformer II of MPK.

## MICROWAVE SPECTRUM

**Experimental Setup.** The microwave spectrum of MPK was recorded using modified versions of the molecular jet Fourier transform microwave spectrometers described in Ref. 35 and 36 operating in a frequency range from 2 to 40 GHz. The substance was purchased from Alfa Aesar GmbH & Co KG, Karlsruhe, Germany. The stated purity is more than 99 % and no further purifications were carried out. A mixture of 1 % MPK in helium at a stagnation pressure of 100 kPa was expanded through a pulsed nozzle into the cavity. At the beginning, a series of overlapping spectra from 9.9 to 14.4 GHz was recorded in a step width of 0.25 MHz. In a second step, all fitted signals were remeasured at higher resolution.

**Spectral Analysis.** The splittings between the (00) and (10) species arising from the acetyl methyl rotation with a calculated barrier height of about  $100\text{ cm}^{-1}$  to  $230\text{ cm}^{-1}$  (see the section on the *Barriers to Internal Rotation*) range from some MHz up to several GHz, and the (00) and (10) species are well-separated in the broadband scan. The additional splittings of these two components into the (00), (01) species and the (10), (11), (12) species, respectively, due to the butyryl methyl group are very small and range from several 100 kHz down to less than 4 kHz. These narrow splittings correspond well with the rather high calculated barrier of around  $1000\text{ cm}^{-1}$ . However, they are not resolvable for all transitions, especially in case of the (00) and (01) species. Figure 5 and 6 illustrate a typical spectrum of the  $4_{13} \leftarrow 3_{12}$  rotational transition of conformer II. Some transitions exhibit further additional splittings, which might be caused by spin-spin or spin-rotation coupling of the hydrogen atoms. All of these effects cause significant enlargement of the line widths. The average line width is 45 kHz (FWHH), but the variation for individual lines is large. Consequently, the measurement accuracy of the line position is only approximately 7-8 kHz for some lines, while other lines have a much better accuracy. For the whole data set, we use a measurement accuracy of 4.5 kHz, which corresponds to 1/10 of the average line width.

## Spectral Assignments and Fits.

**Conformer II.** To start the spectrum analysis, the internal rotation effects were neglected and MPK was considered as a rigid rotor. The rotational constants of conformer II calculated at the MP2/6-311++G(d,p) level of theory given in Table 1 were inserted in the *XIAM* program<sup>27</sup> in its rigid-rotor mode to predict the frequencies of the (00) species for a comparison with the experimental broadband scan. Though quantum chemistry calculated that the dipole moment component in *a*-direction is much smaller than that in *b*-direction (see Table 1), we still began with searching for *a*-type transitions, due to their characteristic pattern. Several *a*-type lines could be identified straightforwardly in the experimental spectrum. Based on this assignment, further *a*-type and afterwards *b*-type lines could be assigned. This enabled us to predict the whole rigid-rotor spectrum with sufficient accuracy to find all remaining (00) species lines in the frequency range from 3 to 40 GHz.

As a next step, the internal rotation of the acetyl methyl group was considered with a prediction of the (00) and (10) species transitions. The starting value for the angle between the internal rotor axis and the principal axis *a* was taken from *ab initio* results at the MP2/6-311++G(d,p) level. The initial  $V_3$  potential was set to  $183\text{ cm}^{-1}$ , which is the value found in methyl ethyl ketone.<sup>11</sup> By comparing the theoretical and experimental broadband scan, the assignment was straightforward for some *a*-type transitions, where the splittings between the (00) and (10) species were relatively small (less than 50 MHz). The assignment of *b*-type lines with much larger splittings was more difficult, however, successful by trial and error. A total of 174 torsional lines were finally assigned and fitted with the *XIAM* program to a root-mean-square (rms) deviation of 8.7 kHz, given as Fit *XIAM*(1Top) in Table 2. It is notable that this deviation is only achievable by fitting the three higher order parameters  $D_{\text{pi}2J}$ ,  $D_{\text{pi}2K}$  and  $D_{\text{pi}2-}$ . The barrier to internal rotation is  $188.3843(50)\text{ cm}^{-1}$ . Since the analysis only includes transitions in the ground torsional state, a strong correlation between  $V_3$  and  $F_0$  is

present. Therefore,  $F_0$  was fixed to 158 GHz, corresponding to  $I_\alpha = 3.1986 \text{ u}\text{\AA}^2$ , a value often found for methyl groups.

The *BELGI-C<sub>s</sub>*<sup>28</sup> fit of the same data set with 14 parameters decreased the deviation value to 3.5 kHz. The starting values of the rotational constants  $A$ ,  $B$  and  $C$  were derived by a transformation of the values obtained from Fit XIAM(1Top) into the rho axis system. The initial values of the internal rotation parameters  $V_3$ ,  $\rho$  and  $F$  were taken directly from Fit XIAM(1Top), whereby only  $V_3$  and  $\rho$  were fitted and  $F$  was fixed to the XIAM value. The off-diagonal element  $D_{ab}$  (multiplying the off-diagonal  $\{\mathbf{P}_a, \mathbf{P}_b\}$  term) of the moment of inertia tensor was present due to the use of the nonprincipal axis system and was calculated from the results of the XIAM(1Top) fit. To achieve the measurement accuracy, three centrifugal distortion constants and five higher order parameters ( $F_V$ ,  $L_V$ ,  $k_1$ ,  $k_2$ , and  $c_I$ ) were also floated. The *BELGI-C<sub>s</sub>* parameters in the rho axis system are available in Table S6 in the ESI. Parameters, which can be transformed into the principal axis system are summarized as Fit BELGI-C<sub>s</sub> in Table 2. A list of all fitted transition is given in Table S7.

**Conformer I.** After conformer II was assigned, a large number of lines remained in the scan. For the assignment process of conformer I, the same scheme as mentioned in the section on the *Conformer II* was applied. Nevertheless, it turned out to be much more difficult, because the predicted spectrum did not match at first the experimental one. After many trials and errors, the rigid rotor spectrum containing the (00) species could be assigned. Subsequently, we attempted to assign the (10) species. Also here, the angles between the internal rotor axis and the principal axes from *ab initio* and the  $V_3$  potential of  $188 \text{ cm}^{-1}$  found for conformer II were used as initial values. However, again, no agreement between the theoretical and the experimental spectra could be observed. Hence, the barrier height was increased in steps of  $10 \text{ cm}^{-1}$  until the calculated spectrum reasonably matched the experimental one at a surprisingly

high value of  $238.145(21) \text{ cm}^{-1}$ . A total of 264 torsional lines were finally assigned and fitted with the *XIAM* program to a rms deviation of 21.0 kHz.

The *BELGI-C<sub>1</sub>*<sup>29</sup> code improved the deviation of the same data set to 4.6 kHz with 16 parameters, where in this case, parameters such as  $D_{aci}$  allowed for molecules with  $C_1$  symmetry were included. A summary of all molecular parameters for the Fit *XIAM*(1Top) and Fit *BELGI-C<sub>1</sub>* is also given in Table 2, a list of all fitted transition in Table S8 in the ESI. The *BELGI-C<sub>1</sub>* parameters in the rho axis system are available in Table S9.

**Two-Top Fits.** Splittings due to internal rotation of the butyryl methyl group are small but resolvable for about half of the rotational transitions. In a *XIAM* two-top fit, the (01), (11) and (12) species lines were added and thereby, the number of lines increased to 294 for conformer II and 388 for conformer I (see Fit *XIAM*(2Tops) in Table 2). The experimental deduced barrier height of the butyryl methyl group is  $978.7(68) \text{ cm}^{-1}$  for conformer I and  $1031.6(21) \text{ cm}^{-1}$  for conformer II, which is close to the calculated values (see the section on the *Barriers to Internal Rotations*). For both conformers, the  $F_0$  value of the butyryl methyl group was also fixed to 158 GHz as for the acetyl methyl group. The angles between the butyryl methyl rotor axis and the principal axes could not be fitted and were fixed to the *ab initio* values derived from the optimized geometries mentioned in the section on the *Conformational Analysis*. The rms deviations of the two-top fits are slightly higher than those of the one-top fits. If the (01), (11) and (12) species lines are referred to the position of the respective (00) or (10) line, the rms deviation of such a relative *XIAM* fit is 8.0 kHz for conformer I and 7.0 kHz for conformer II by fitting only one parameter, the barrier height of the butyryl methyl group. The residuals of these absolute and relative two-top fits are listed in Table S10 and Table S11 in the ESI.

## RESULTS AND DISCUSSION

According to the *XIAM* fits, the torsional barrier of the acetyl methyl group is 238.145(21)  $\text{cm}^{-1}$  for conformer I and 188.3843(50)  $\text{cm}^{-1}$  for conformer II. The values obtained by *BELGI* agree within 1 %, while improving the standard deviations to measurement accuracy for both conformers (see Table 2). Both *XIAM* fits show much larger standard deviations due to the limited number of parameters available in this program, which is proved by some branches of lines with systematic deviations. We notice that the residuals of some lines in the *BELGI* fits are higher than the average deviation, because these transitions show large splittings arising from the internal rotation of the butyryl methyl group, which are not considered by the *BELGI* model.

Conformer I with the barrier to internal rotation of the acetyl methyl group of about 238  $\text{cm}^{-1}$  exhibits a bent structure with  $C_1$  symmetry, where the  $\gamma$ -carbon of the propyl chain is in a nearly synclinal position. For conformer II, the barrier height of 188.384  $\text{cm}^{-1}$  is much smaller. The structure of conformer II is pseudo- $C_s$ , where the entire propyl chain is tilted out of the heavy atom acetyl plane by about  $10^\circ$  (see the section on the *Conformational Analysis*). By comparing the results of the present work with other ketones investigated in the literature, we found a scheme with two different classes. The first class contains ketones featuring a pseudo- $C_s$  structure where the torsional barrier is always close to 180  $\text{cm}^{-1}$ . Examples are conformer II of MPK (188.384  $\text{cm}^{-1}$ ) and methyl ethyl ketone (183.170  $\text{cm}^{-1}$ ).<sup>11</sup> Even, if the alkyl chain is branched, as in the case of methyl neopentyl ketone, the barrier height seems to be almost unaffected (174.1  $\text{cm}^{-1}$ ).<sup>8</sup> The second class comprises molecules with a real  $C_1$  symmetry and a higher barrier height of about 240  $\text{cm}^{-1}$ . Conformer I of MPK (238.14  $\text{cm}^{-1}$ ), allyl acetone (225  $\text{cm}^{-1}$ )<sup>37</sup> and methyl isobutyl ketone (250  $\text{cm}^{-1}$ )<sup>38</sup> belong to this class. To verify and expand this “two class concept”, further methyl alkyl ketones will be investigated in the future.

Geometry optimizations of conformer II have shown that the propyl group is slightly tilted out of the plane containing the acetyl group. Nevertheless, despite carefully searching for *c*-type transitions, none of them were found. The absence of *c*-type transitions suggests the following possibilities: (i) The real structure features  $C_s$  symmetry. (ii) The real structure is not  $C_s$ , however, the dipole moment component in *c*-direction is too small and thus *c*-type lines are too weak to be detected with the sensitivity of the spectrometer. (iii) The enantiomers are separated by a low barrier and the tunneling ground state is above this barrier causing an *effective*  $C_s$  geometry. In this case the expectation value of the dipole moment in *c* direction would be zero. Indeed, calculations at the MP2/6-311++G(d,p) level of theory yield a tunneling barrier height of  $15.0\text{ cm}^{-1}$ , while the ground state lies at about  $30\text{ cm}^{-1}$ . The  $V_6$  contribution in the potential of the acetyl methyl group of conformer II, as presented in Figure 4, would generate additional splittings of the A and E torsional species of the threefold rotor, if the lowest torsional level lay below the local maxima, as it is for example the case for pinacolone.<sup>18</sup> This is clearly not the case for MPK because no additional splittings rather than those of the butyryl methyl torsion are observed in the spectrum. A further support for a  $C_s$  or an *effective*  $C_s$  symmetry is that the fit achieved with *BELGI-C<sub>s</sub>*, which reproduced the experimental data within measurement accuracy, did not require any out-of-plane terms. Finally, the inertial defect  $\Delta_c = I_c - I_a - I_b$  of  $-12.688\text{ u\AA}^2$  confirms that the heavy atom skeleton is planar. This value is almost the same as that found in methyl butyrate ( $\Delta_c = -13.018\text{ u\AA}^2$ ),<sup>16</sup> which also contains four pairs of out-of-plane hydrogen atoms.

The observed rotational constants of conformer II agree within approximately 1 % with the calculated values obtained at different method and basis set combinations (see Table S3 in the ESI). They differ more significantly for conformer I, especially for the A rotational constant (see Table S2 in the ESI). At some levels of theory with the MP2 method, the calculated A rotational constant is up to 4 % smaller than the experimental value. The

deviations are in general better with DFT based levels, which is probably due to error compensation.

Most of the lines in the microwave spectrum of MPK were assigned to either conformer I or conformer II. In the range of the broadband scan, which spans 4.5 GHz, only 16 weak lines remained unassigned. They might be due to conformer III or IV of MPK,  $^{13}\text{C}$  isotopologues or impurities.

## CONCLUSIONS

MPK was investigated by quantum chemical calculations and the two energetically most favorable conformers were assigned in the rotational spectrum. The barrier to internal rotation of the acetyl methyl group is about  $238.1\text{ cm}^{-1}$  for conformer I and  $188.4\text{ cm}^{-1}$  for conformer II. These values could be linked to the geometry of the respective conformer. Conformer I features a  $\text{C}_1$  structure, where the  $\gamma$ -carbon of the propyl chain is in an almost synclinal position and conformer II exhibiting a pseudo- $\text{C}_s$  structure, where the propyl chain is tilted out of the heavy atom acetyl plane by approximately  $10^\circ$ . Comparisons with other methyl alkyl ketones yielded that those ketones with  $\text{C}_1$  structure also have acetyl methyl barrier heights of about  $240\text{ cm}^{-1}$ , while those with pseudo- $\text{C}_s$  structure exhibit barriers to internal rotation of approximately  $180\text{ cm}^{-1}$ . Based on this observation, we suggested two different classes of methyl alkyl ketones associated with different torsional barriers. To verify or expand this classification system, further investigation of methyl alkyl ketones have to be carried out.

## ASSOCIATED CONTENT

**Electronic Supporting Information.** Nuclear coordinates in the principal axis system of the conformers, basis set variation, Fourier coefficients of potential energy curves, spectroscopic constants of the *BELGI* fits in the rho axis system, frequency lists. This material is available free of charge via the Internet at <http://pubs.acs.org>.

## AUTHOR INFORMATION

### Corresponding Author

\* Email: lam.nguyen@lisa.u-pec.fr, Tel.: +33 145 17 65 48.

## ACKNOWLEDGMENT

We thank Dr. Layla Tulimat and Jade Turrel for the measurements and calculations they carried out to contribute to this work. Simulations were performed with computing resources granted by RWTH Aachen University under project <rwth0249>.

## REFERENCES

- (1) Tudorie, M.; Kleiner, I.; Hougen, J. T.; Melandri, S.; Sutikdja, L. W.; Stahl, W. A Fitting Program for Molecules with Two Inequivalent Methyl Tops and a Plane of Symmetry at Equilibrium: Application to New Microwave and Millimeter-wave Measurements of Methyl Acetate. *J. Mol. Spectrosc.* **2011**, *269*, 211-225.
- (2) Jelisavac, D.; Cortés Gómez, D. C.; Nguyen, H. V. L.; Sutikdja, L. W.; Stahl, W.; Kleiner, I. The Microwave Spectrum of the *trans* Conformer of Ethyl Acetate. *J. Mol. Spectrosc.* **2009**, *257*, 111-115.
- (3) Sutikdja, L. W.; Stahl, W.; Sironneau, V.; Nguyen, H. V. L.; Kleiner, I. Structure and Internal Dynamics of *n*-Propyl Acetate Studied by Microwave Spectroscopy and Quantum Chemistry. *Chem. Phys. Lett.* **2016**, *663*, 145-149.
- (4) Attig, T.; Sutikdja, L. W.; Kannengießer, R.; Kleiner, I.; Stahl, W. The Microwave Spectrum of *n*-Butyl Acetate. *J. Mol. Spectrosc.* **2013**, *284-285*, 8-15.
- (5) Attig, T.; Kannengießer, R.; Kleiner, I.; Stahl, W. Conformational Analysis of *n*-Pentyl Acetate Using Microwave Spectroscopy. *J. Mol. Spectrosc.* **2013**, *290*, 24-30.

- (6) Attig, T.; Kannengießer, R.; Kleiner, I.; Stahl, W. The Microwave Spectrum of *n*-Hexyl Acetate and Structural Aspects of *n*-Alkyl Acetates. *J. Mol. Spectrosc.* **2014**, *298*, 47-53.
- (7) Van, V.; Stahl, W.; Nguyen, H. V. L. The Structure and Torsional Dynamics of Two Methyl Groups in 2-Acetyl-5-methylfuran as Observed by Microwave Spectroscopy. *Chem. Phys. Chem.* **2016**, *17*, 3223-3228.
- (8) Zhao, Y.; Jin, J.; Stahl, W.; Kleiner, I. The Microwave Spectrum of Methyl Neopentyl Ketone. *J. Mol. Spectrosc.* **2012**, *281*, 4-8.
- (9) Wilcox, D. S.; Shirar, A. J.; Williams, O. L.; Dian, B. C. Additional Conformer Observed in the Microwave Spectrum of Methyl Vinyl Ketone. *Chem. Phys. Lett.* **2011**, *508*, 10-16.
- (10) Groner, P. Experimental Two-dimensional Torsional Potential Function for the Methyl Internal Rotors in Acetone. *J. Mol. Struct.* **2000**, *550-551*, 473-479.
- (11) Nguyen, H. V. L.; Van, V.; Stahl, W.; Kleiner, I. The Effects of Two Internal Rotations in the Microwave Spectrum of Ethyl Methyl Ketone. *J. Chem. Phys.* **2014**, *140*, 214303.
- (12) Nguyen, H. V. L.; Stahl, W. The Effects of Nitrogen Inversion Tunneling, Methyl Internal Rotation, and <sup>14</sup>N Quadrupole Coupling Observed in the Rotational Spectrum of Diethyl Amine. *J. Chem. Phys.* **2011**, *135*, 024310.
- (13) Francke, W.; Lübke, G.; Schröder, W.; Reckziegel, A.; Imperatriz-Fonseca, V.; Kleinert, A.; Engels, E.; Hartfelder, K.; Radtke, R.; Engels, W. Identification of Oxygen Containing Volatiles in Cephalic Secretions of Workers of Brazilian Stingless Bees. *J. Braz. Chem. Soc.* **2000**, *11*, 562-571.
- (14) Bestmann, H. J.; Vostrowsky, O. Chemische Informationssysteme der Natur: Insektenpheromone. *Chem. unserer Zeit* **1993**, *27*, 123-133.

- (15) Boch, R.; Shearer, D. A.; Stone, B. C. Identification of Iso-Amyl Acetate as an Active Component in the Sting Pheromone of the Honey Bee. *Nature* **1962**, *195*, 1018-1020.
- (16) Shearer, D. A.; Boch, R. 2-Heptanone in the Mandibular Gland Secretion of the Honey-bee. *Nature* **1965**, *206*, 530.
- (17) Dreizler, H. Gruppentheoretische Betrachtungen zu den Mikrowellenspektren von Molekülen mit zwei behindert drehbaren dreizählig-symmetrischen Molekülgruppen. *Z. Naturforsch.* **1961**, *16a*, 1354-1367.
- (18) Frisch, M. J.; Trucks, G. W.; Schlegel, H. B.; Scuseria, G. E.; Robb, M. A.; Cheeseman, J. R.; Scalmani, G.; Barone, V.; Mennucci, B.; Petersson G. A. et al. *Gaussian 09*, Gaussian, Inc., Wallingford CT, 2009.
- (19) Ferres, L.; Mouhib, H.; Stahl, W.; Nguyen, H. V. L. Methyl Internal Rotation in the Microwave Spectrum of *o*-Methyl Anisole. *Chem. Phys. Chem.* **2017**, *18*, 1855-1859.
- (20) Van, V.; Stahl, W.; Schwell, M.; Nguyen, H. V. L. Gas-phase Conformations of 2-Methyl-1,3-dithiolane Investigated by Microwave Spectroscopy. *J. Mol. Struct.* **2018**, *1156*, 348-352.
- (21) Van, V.; Bruckhuisen, J.; Stahl, W.; Ilyushin, V.; Nguyen, H. V. L. The Torsional Barriers of Two Equivalent Methyl Internal Rotations in 2,5-Dimethylfuran Investigated by Microwave Spectroscopy. *J. Mol. Spectrosc.* **2018**, *343*, 121-125.
- (22) Hernandez-Castillo, A. O.; Abeysekera, C.; Hays, B. M.; Kleiner, I.; Nguyen, H. V. L.; Zwier, T. S. Conformational Preferences and Internal Rotation of Methyl Butyrate by Microwave Spectroscopy. *J. Mol. Spectrosc.* **2017**, *337*, 51-58.
- (23) Nguyen, H. V. L.; Stahl, W. The Rotational Spectrum of Diethyl Ketone. *Chem. Phys. Chem.* **2011**, *12*, 1900-1905.

- (24) Zhao, Y.; Nguyen, H. V. L.; Stahl, W.; Hougen, J. T. Unusual Internal Rotation Coupling in the Microwave Spectrum of Pinacolone. *J. Mol. Spectrosc.* **2015**, *318*, 91-100.
- (25) Jabri, A.; Van, V.; Nguyen, H. V. L.; Stahl, W.; Kleiner, I. Probing the Methyl Torsional Barriers of the *E* and *Z* Isomers of Butadienyl Acetate by Microwave Spectroscopy. *Chem. Phys. Chem.* **2016**, *17*, 2660-2665.
- (26) Ferres, L.; Stahl, W.; Nguyen, H. V. L. The Molecular Structure of Phenetole Studied by Microwave Spectroscopy and Quantum Chemical Calculations. *Mol. Phys.* **2016**, *114*, 2788-2793.
- (27) Hartwig, H.; Dreizler, H. The Microwave Spectrum of *trans*-2,3-Dimethyloxirane in Torsional Excited States. *Z. Naturforsch.* **1996**, *51a*, 923-932.
- (28) Hougen, J. T.; Kleiner, I.; Godefroid, M. Selection Rules and Intensity Calculations for a  $C_s$  Asymmetric Top Molecule Containing a Methyl Group Internal Rotor. *J. Mol. Spectrosc.* **1994**, *163*, 559-585.
- (29) Kleiner, I.; Hougen, J. T. Rho-axis-method Hamiltonian for Molecules Having One Methyl Rotor and  $C_1$  Point-group Symmetry at Equilibrium. *J. Chem. Phys.* **2003**, *119*, 5505-5509.
- (30) Herbst, E.; Messer, J. K.; De Lucia, F. C.; Helminger, P. A New Analysis and Additional Measurements of the Millimeter and Submillimeter Spectrum of Methanol. *J. Mol. Spectrosc.* **1984**, *108*, 42-57.
- (31) Kleiner, I. Asymmetric-top Molecules Containing One Methyl-like Internal Rotor: Methods and Codes for Fitting and Predicting Spectra. *J. Mol. Spectrosc.* **2010**, *260*, 1-18.

- (32) Ferres, L.; Stahl, W.; Kleiner, I.; Nguyen, H. V. L. The Effect of Internal Rotation in *p*-Methyl Anisole Studied by Microwave Spectroscopy. *J. Mol. Spectrosc.* **2018**, *343*, 44-49.
- (33) Eibl, K.; Kannengießer, R.; Stahl, W.; Nguyen, H. V. L.; Kleiner, I. Low Barrier Methyl Rotation in 3-Pentyn-1-ol as Observed by Microwave Spectroscopy. *Mol. Phys.* **2016**, *114*, 3483-3489.
- (34) Nguyen, H. V. L.; Jabri, A.; Van, V.; Stahl, W. Methyl Internal Rotation in the Microwave Spectrum of Vinyl Acetate. *J. Phys. Chem. A* **2014**, *118*, 12130-12136.
- (35) Grabow, J.-U.; Stahl, W.; Dreizler, H. A Multioctave Coaxially Oriented Beam-resonator Arrangement Fourier-transform Microwave Spectrometer. *Rev. Sci Instrum.* **1996**, *67*, 4072-4084.
- (36) Merke, I.; Stahl, W.; Dreizler, H. A Molecular Beam Fourier Transform Microwave Spectrometer in the Range 26.5 to 40 GHz. Tests of Performance and Analysis of the D- and <sup>14</sup>N-hyperfine Structure of Methylcyanide-d<sub>1</sub>. *Z. Naturforsch.* **1994**, *49a*, 490-496.
- (37) Tulimat, L.; Mouhib, H.; Kleiner, I.; Stahl, W. The Microwave Spectrum of Allyl Acetone. *J. Mol. Spectrosc.* **2015**, *312*, 46-50.
- (38) Zhao, Y.; Stahl, W.; Nguyen, H. V. L. Ketone Physics – Structure, Conformations, and Dynamics of Methyl Isobutyl Ketone Explored by Microwave Spectroscopy and Quantum Chemical Calculations. *Chem. Phys. Lett.* **2012**, *545*, 9-13.

## FIGURES

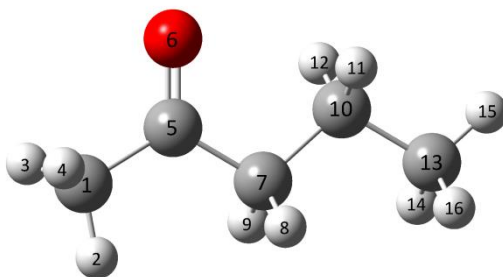


**Figure 1.** Atom numbering of methyl propyl ketone in a  $C_s$  reference configuration. The hydrogen atoms are in white, the carbon atoms in grey and the oxygen atom is in red.

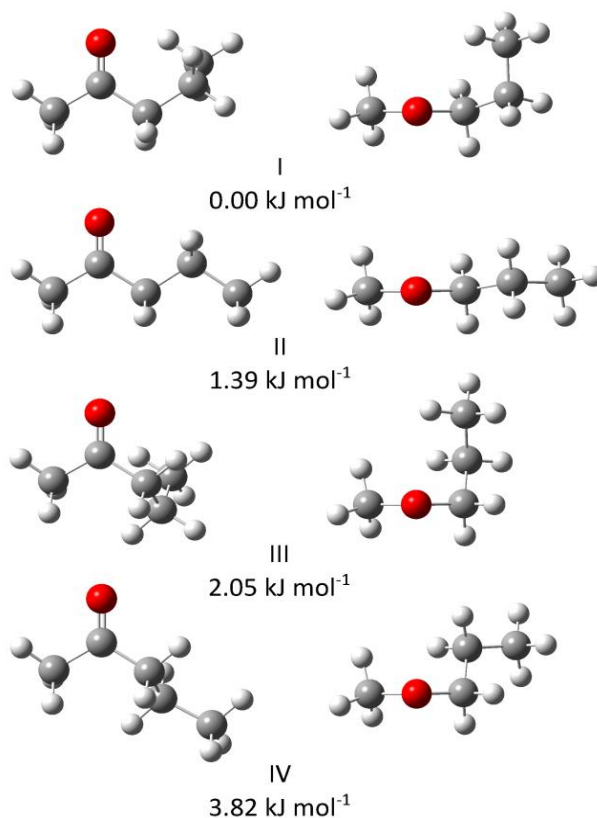


**Figure 2.** Geometries of the four conformers of methyl propyl ketone calculated at the MP2/6-311++G(d,p) level of theory. Left hand side: view on the C–CO–C plane; Right hand side: view along the O=C bond. The relative energies refer to the absolute energy of conformer I with  $E = -271.047861$  Hartree.

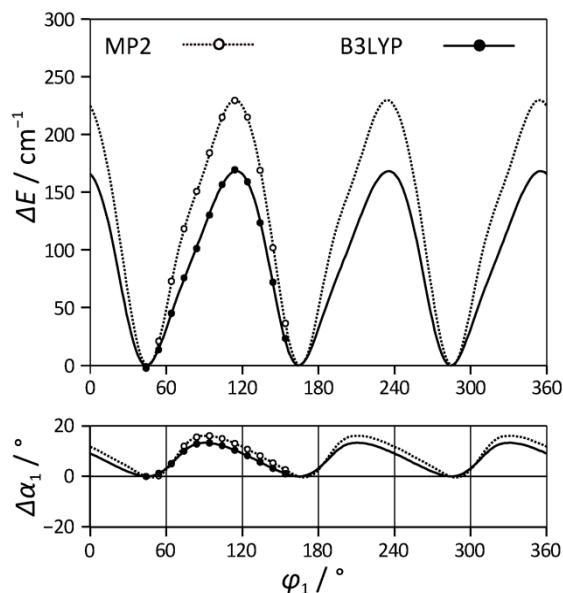


**Figure 3.** Upper figure: Potential energy curve of the acetyl methyl group of conformer I of methyl propyl ketone obtained by varying the dihedral angle  $\varphi_1 = \angle(\text{H}_2, \text{C}_1, \text{C}_5, \text{C}_7)$  with a step width of  $10^\circ$  and parameterizing the resulting energies with a Fourier expansion. The energies are calculated at the MP2/6-311++G(d,p) and B3LYP/6-311++G(d,p) levels of theory and are given relative to that of the lowest energy conformations. Lower figure: Deviation of the dihedral angle  $\alpha_1 = \angle(\text{C}_1, \text{C}_5, \text{C}_7, \text{C}_{10})$  depending on the position of the acetyl methyl group.  $\Delta\alpha_1$  is given relative to a value of  $\alpha_1 = 161.4^\circ$  (MP2) and  $165.9^\circ$  (B3LYP).

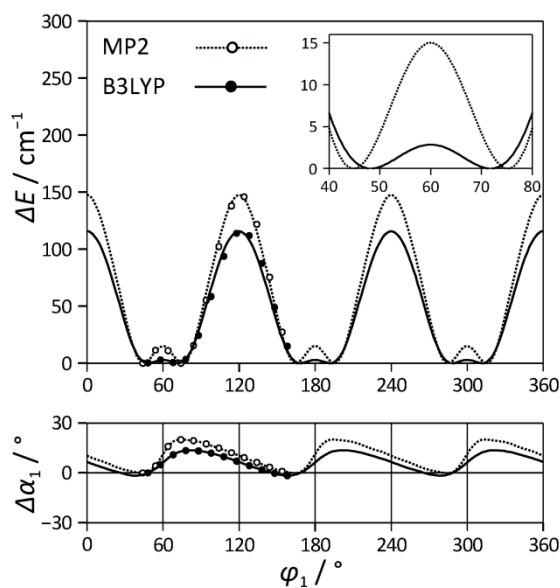


**Figure 4.** Upper figure: Potential energy curve of the acetyl methyl group of conformer II of methyl propyl ketone obtained by varying the dihedral angle  $\phi_1 = \angle(\text{H}_2, \text{C}_1, \text{C}_5, \text{C}_7)$  with a step width of  $10^\circ$  and parameterizing the resulting energies with a Fourier expansion. The energies are calculated at the MP2/6-311++G(d,p) and B3LYP/6-311++G(d,p) levels of theory and are given relative to that of the lowest energy conformations. Inset: The double minimum located between  $\phi_1 = 40^\circ$  and  $80^\circ$  is depicted in an enlarged scale, where  $\phi_1$  was varied in a step width of  $1^\circ$ . Lower figure: Deviation of the dihedral angle  $\alpha_1 = \angle(\text{C}_1, \text{C}_5, \text{C}_7, \text{C}_{10})$  depending on the position of the acetyl methyl group.  $\Delta\alpha_1$  is given relative to a value of  $\alpha_1 = 170.0^\circ$  (MP2) and  $174.0^\circ$  (B3LYP).

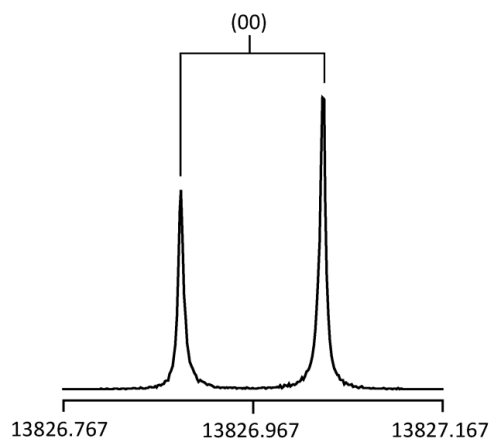


**Figure 5.** A high resolution measurement of the (00) species of the  $4_{13} \leftarrow 3_{12}$  transition of conformer II found at 13826.9668 MHz. The splitting indicated by the brackets is caused by the Doppler effect. The splitting in (00) and (10) species is not resolvable. For this spectrum 85 decays were co-added.

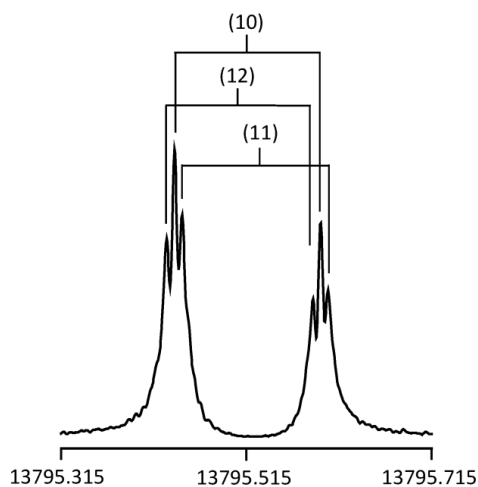


**Figure 6.** A high resolution measurement of the (10) (13795.5167 MHz), (11) (13795.5239 MHz) and (12) (13795.5082 MHz) species of the  $4_{13} \leftarrow 3_{12}$  transition of conformer II. The splittings indicated by the brackets are caused by the Doppler effect. For this spectrum 301 decays were co-added.

TABLES

**Table 1.** Relative energies at equilibrium and with zero point corrections (in  $\text{kJ}\cdot\text{mol}^{-1}$ ), rotational constants (in GHz), dipole moment components (in Debye), and optimized dihedral angles  $\alpha_1 = \angle(\text{C}_1, \text{C}_5, \text{C}_7, \text{C}_{10})$ ,  $\alpha_2 = \angle(\text{C}_5, \text{C}_7, \text{C}_{10}, \text{C}_{13})$  (in degree) of the four conformers (I – IV) of methyl propyl ketone calculated at the MP2/6-311++G(d,p) level of theory.

	$E^a$	ZPE <sup>b</sup>	<i>A</i>	<i>B</i>	<i>C</i>	$ \mu_a $	$ \mu_b $	$ \mu_c $	$\alpha_1$	$\alpha_2$
<b>I</b>	0	0	6.301	2.169	1.975	0.26	3.17	0.59	161.4	-69.5
<b>II</b>	1.39	0.69	8.264	1.797	1.534	0.53	3.21	0.04	170.1	179.0
<b>III</b>	2.05	2.79	5.149	2.372	2.203	1.99	2.91	0.74	59.4	59.8
<b>IV</b>	3.82	4.18	7.246	1.856	1.612	2.42	2.63	0.78	60.3	176.0
<b>Exp. I<sup>c</sup></b>			<b>6.554</b>	<b>2.148</b>	<b>1.927</b>					
<b>Exp. II<sup>c</sup></b>			<b>8.336</b>	<b>1.795</b>	<b>1.534</b>					

<sup>a</sup> Referring to the absolute energy of  $E = -271.047861$  Hartree of conformer I. <sup>b</sup> Referring to the zero point corrected energy of  $E = -270.905256$  Hartree of conformer I. <sup>c</sup> Experimentally deduced rotational constants obtained from the XIAM(1Top) fit, see Table 2.

**Table 2.** Molecular parameters of conformer I and conformer II of methyl propyl ketone obtained by the *BELGI* program,<sup>28,29</sup> as well as by the *XIAM* program<sup>27</sup> including one or two internal rotors, respectively. All parameters refer to the principal axis system.

Parameter	Unit	Conformer I			Conformer II		
		BELGI-C <sub>1</sub> <sup>a</sup>	XIAM(1Top) <sup>b</sup>	XIAM(2Tops) <sup>b</sup>	BELGI-C <sub>s</sub> <sup>a</sup>	XIAM(1Top) <sup>b</sup>	XIAM(2Tops) <sup>b</sup>
<i>A</i>	GHz	6.49803(43)	6.5541414(19)	6.5541419(20)	8.36552(20)	8.3356770(14)	8.3356766(15)
<i>B</i>	GHz	2.15380(13)	2.14826850(56)	2.14827148(59)	1.796710(37)	1.79533613(25)	1.79535122(28)
<i>C</i>	GHz	1.929377(61)	1.92693152(37)	1.92693027(38)	1.5352434(38)	1.53407498(26)	1.53405998(29)
$\Delta_J$	kHz		0.9143(23)	0.9161(22)	0.1293(07)	0.1409(16)	0.1412(15)
$\Delta_{JK}$	kHz		-2.7328(97)	-2.7422(98)		1.143(14)	1.147(14)
$\Delta_K$	kHz		25.365(63)	25.419(58)		7.016(46)	7.023(47)
$\delta_J$	kHz		-0.07906(39)	-0.07924(41)		0.02240(56)	0.02259(65)
$\delta_K$	kHz		4.282(26)	4.286(28)		0.325(40)	0.352(46)
$F_{0,1}$	GHz	156.61(11)	158.0 (fixed)	158.0 (fixed)	164.405(60)	158.0 (fixed)	158.0 (fixed)
$V_{3,1}$	cm <sup>-1</sup>	238.219(48)	238.144(21)	238.192(22)	186.237(22)	188.3842(50)	188.6959(54)
$\angle(i_1,a)$	°	26.848(13)	26.911(30)	26.899(31)	36.9974(25)	37.0597(50)	37.0688(54)
$\angle(i_1,b)$	°	108.917(10)	109.134(44)	109.115(46)	126.9974(25)	127.0597(50)	127.0688(54)
$\angle(i_1,c)$	°	71.6748(88)	71.814(44)	71.810(46)	90.0 (fixed)	90.0 (fixed)	90.0 (fixed)
$D_{\text{pi}2J,1}$	MHz		0.4323(25)	0.4258(24)		0.06452(53)	0.06477(58)
$D_{\text{pi}2K,1}$	MHz		-5.107(16)	-5.103(16)		-1.2754(60)	-1.2849(62)
$D_{\text{pi}2-,1}$	MHz		-1.201(30)	-1.216(32)		0.02099(31)	0.02154(35)
$V_{3,2}$	cm <sup>-1</sup>			978.7(68) <sup>c</sup>			1031.6(21) <sup>d</sup>
$N^e$	–	264	264	388	174	174	294
$N((00)/(10))^f$	–	141/123	141/123	141/123	83/91	83/91	83/91
$N((01)/(11)/(12))^f$	–			0/62/62			22/49/49
$\sigma^g$	kHz	4.6	21.0	23.2	3.5	8.7	11.2

<sup>a</sup> Parameters obtained by transformation from rho axis system to principal axis system. <sup>b</sup> Watson's A reduction and I<sup>r</sup> representation were used. <sup>c</sup> Internal rotation parameters of the second rotor are fixed to  $F_{0,2} = 158.0$  GHz,  $\angle(i_2,a) = 110.5^\circ$ ,  $\angle(i_2,b) = 68.6^\circ$  and  $\angle(i_2,c) = 30.4^\circ$ . <sup>d</sup> For this conformer,  $F_{0,2} = 158.0$  GHz,  $\angle(i_2,a) = 153.0^\circ$ ,  $\angle(i_2,b) = 117.0^\circ$  and  $\angle(i_2,c) = 90.0^\circ$ . <sup>e</sup> Total number of lines. <sup>f</sup> Number of lines of each symmetry species. <sup>g</sup> Rms deviation of the fit.

## TOC Graphic

